JOURNAL OF GEOPHYSICAL RESEARCH, VOL. 104, NO. D10, PAGES 12,077–12,084, MAY 27, 1999

In situ observations of contrail microphysics and implications for their radiative impact

Michael R. Poellot

Department of Atmospheric Sciences, University of North Dakota, Grand Forks

W. Patrick Arnott and John Hallett

Atmospheric Science Center, Desert Research Institute, Reno, Nevada

Abstract. In this study we present the microphysical characteristics of 21 jet contrail clouds sampled in situ and examine the possible effects of exhaust on natural cirrus and radiative effects of contrails. Microphysical samples were obtained with Particle Measuring Systems (PMS) 2D-C, 1D-C, and FSSP probes. About one half of the study contrails were generated by the sampling aircraft, a Cessna Citation, primarily at times of 3–15 min after generation; the source and age of the others is unknown. On average, the contrails contained particles of mean diameter of the order of 10 μm in concentrations exceeding 10,000 L^{-1}. Contrails embedded in natural cirrus appeared to have little effect on the natural cloud microphysics. Anomalous diffraction theory was used to model radiative properties of sampled contrails. The contrail cirrus showed considerably more spectral variation in extinction and absorption efficiencies than natural cirrus because of the large numbers of small crystals in contrails. Embedded contrails also displayed greater emissivity and emission than natural cirrus and a greater spectral variation in transmission.

1. Introduction

Increasing levels of air traffic have raised concerns about the potential effects of aircraft exhaust on the climate. One possible mechanism for effect is through changes in the radiative budget of the atmosphere resulting from the generation of contrail clouds or the modification of natural cirrus clouds by exhaust products. The net effect of contrail clouds would depend on their duration, areal coverage, and radiative properties. With the rapid growth of commercial jet traffic in the 1960s, the frequency and areal coverage of persistent contrail cirrus became quite marked [e.g., *Changnon et al.*, 1980]. The generation of "artificial cirrus" has even been proposed as a means of intentionally reducing surface temperatures [*Johnson et al.*, 1969]. A possible contribution by contrails to climate change has been noted by several authors [e.g., *Liou et al.*, 1990; *Sassen*, 1997; *Smith et al.*, 1998], but it is not clear whether the net effect, if any, would be warming or cooling. The modification of natural cirrus may result from the nucleation of additional ice particles on exhaust aerosols or through increased competition between contrail and natural ice for available water vapor. For contrails that form within natural cirrus clouds, the competition for atmospheric water vapor may limit the maximum size of particles within the plume, as it did within the core of a contrail plume reported by *Heymsfield et al.* [1998].

The uncertainty surrounding climatic effects of contrails is related in part to a dearth of adequate sampling of their radiative impact and microphysical characteristics. Airborne radiometric measurements by *Kuhn* [1970] indicated locally strong (12%) reductions in net downwelling radiation below contrails. A rather extensive surface-based study of contrail effects over Illinois also showed locally significant radiative effects [*Wendland and Semonin*, 1982]. The radiative impact of an aircraft contrail is dependent to a large degree on the cloud microphysics as the infrared and solar forcing are strongly dependent on particle numbers and sizes. In one of the few in situ microphysical studies to date, *Knollenberg* [1972] studied the characteristics of a persistent contrail and its effects on the local water vapor budget. Measurements of particle sizes and numbers were limited to particles larger than ~100 μm. A more recent sampling of four contrails by *Gayet et al.* [1996a] found significant differences between the microphysical characteristics of natural and contrail cirrus. Using probes with a minimum size resolution of 25 μm, large concentrations of small particles (<100 μm in diameter) were detected in the contrails. Near-field measurements of contrail microphysics by *Baumgardner and Cooper* [1994] characterized particle distributions to submicron sizes with evidence for significant concentrations of particles between 1 and 10 μm. Other evidence for small mean particle sizes in contrails has been seen in remote sensing by satellite [e.g., *Gothe and Grassl*, 1993] and by visual observation [*Sassen et al.*, 1989]. Most recently, the Subsonic Aircraft Contrail and Cloud Effects Special Study (SUCCESS) [*Toon and Miake-Lye*, 1998] was conducted in 1996 to learn more about the character of aircraft exhaust and contrail clouds. Analyses of both in situ [e.g., *Heymsfield et al.*, 1998] and remote sensing measurements [e.g., *Minnis et al.*, 1998] found that contrails initially contain large numbers of small particles. Under favorable (humid) conditions the particles grow through vapor diffusion as they age and take on the characteristics of natural cirrus.

The impact of the exhaust aerosol upon the atmosphere is nearly instantaneous when conditions are favorable for contrail formation. *Karcher et al.* [1996] argue that the nuclei for the contrail ice particles are formed primarily through the interaction of soot and sulfuric acid produced by combustion. How-

Copyright 1999 by the American Geophysical Union.

Paper number 1999JD900109.
0148-0227/99/1999JD900109$09.00

Table 1. Citation Instrumentation

Parameter	Probe	Range
Temperature	Rosemount total temperature	−65°C to +50°C
Dew point	EG&G cooled mirror	−50°C to +70°C
Pressure	Rosemount	0–1034 mbar
Cloud particles	PMS 2D-C optical array	33–1056 μm
	PMS FSSP-100	2–47 μm
	PMS 1D-C optical array	20–600 μm
Condensation nuclei ($D > 0.01$ μm)	TSI 3760 alcohol condensing	0–10^4 cm^{-3}

ever, *Twohy and Gandrud* [1998] and *Jensen et al*. [1998] suggest that a significant number of ambient aerosol particles may also act as ice nuclei within the plume. As the exhaust plume ages, the nucleating effects of soot or other exhaust products are less certain. *Schuman et al*. [1996] and *Hudson and Xie* [1998] suggest that these aerosols may remain active as cloud condensation or ice nuclei in the upper troposphere and influence the subsequent formation of cirrus clouds. *Pueschel et al*. [1997] have argued that even in the absence of soot, sulfuric acid aerosol may later take on water, dilute, and then freeze homogeneously. These small ice particles may then be of a sufficient size and number to have a significant effect on radiative transfer.

The present study examines the in situ data from 21 contrails sampled at altitudes from 9.3 to 12.5 km and temperatures of −47°C to −66°C. The microphysical characteristics of the contrails, which occurred in both clear and cloudy air, are presented and compared with natural cirrus properties. Distributions of atmospheric aerosol are also examined along with the cloud microphysics to look for possible exhaust effects. Computations of the wavelength-dependent radiative properties of the sampled particle distributions are then presented. Finally, the climatic implications of these findings are discussed.

2. Data

The measurements were taken with probes mounted on the University of North Dakota Cessna Citation aircraft as it was flown on two separate field programs. The first program was the First International Satellite Cloud Climatology Program Region Experiment (FIRE) Cirrus Intensive Field Observations (IFOs) II, which was conducted over southeastern Kansas during late fall of 1991. Flight profiles of the Citation were designed to investigate the structure of natural cirrus and consisted largely of step-up and step-down racetrack patterns. While it was not the intention of these missions to sample aircraft contrail clouds, there were a number of occasions when the Citation penetrated its own exhaust or that of other transient aircraft. The second field study took place over the Atmospheric Radiation Measurement (ARM) Program site in northern Oklahoma during April 1994. These operations were conducted to provide in situ measurements of various atmospheric conditions for comparison with remote sensors. Intentional contrail penetrations were made during one of the missions, and the Citation sampled its own contrail inadvertently on another.

The Citation carried a similar suite of instrumentation for both projects; a subset of sensors relevant to this study is given in Table 1. State-of-the-atmosphere variables were measured with standard instrumentation; unfortunately, the measurements of water vapor were somewhat uncertain because the hygrometer was operating near its lower-temperature limit and will not be presented here. The CN counter data were adjusted for diffusional losses, and a correction was applied to account for reduced counting efficiency at low pressures reported by *Zhang and Liu* [1991]. Because of electronic response at the relatively high sampling speeds, the Particle Measuring System (PMS) 2D-C probe had an effective lower size threshold of 66 μm and the 1D-C a threshold of 40 μm.

The FSSP is designed and calibrated to measure liquid water spheres, and its response to ice particles is uncertain [e.g., *Gardiner and Hallett*, 1985], especially in high concentrations of larger vapor-grown crystals. However, while it is unlikely that the contrails contained any liquid water, there is evidence that the FSSP can provide quantitative estimates of the numbers and sizes of small ice particles when few large particles are present. This has been suggested in a previous study of natural cirrus by *Heymsfield and Platt* [1984] and in the use of modified versions of the FSSP-100 [*Knollenberg et al*., 1993; *Baumgardner et al*., 1992]. *Pueschel et al*. [1997] used FSSP data to size and count small ice crystals in tropical cirrus, supported by comparisons with replicator data. In polar stratospheric clouds, *Baumgardner et al*. [1989] estimated errors in FSSP-derived concentrations of around 40% and in sizing of about 20%. *Gayet et al*. [1996b] also concluded that the FSSP appears to provide quantitative information about contrail cloud microphysics, probably because the particles tend to be compact and quasi-spherical. They caution, however, that significant sizing and counting errors may occur when sampling larger, nonspherical ice crystals; the quality of overlap with 2D-C spectral data is a measure of the reliability of the FSSP data. Although the FSSP and 2D-C size spectra from the Citation do not directly overlap, the 2D-C data can be extrapolated with the help of data from the 1D-C probe to estimate the fit with the FSSP.

The above studies support using the FSSP data to quantitatively describe the sampled contrails, with consideration for the measurement uncertainties. Figure 1 shows a size distribution from FSSP data for contrail *F*. This contrail was isolated (in clear air), and no larger particles were detected by either the 2D-C or the 1D-C probes. It is uncertain whether the roll-off of counts in the first channel (2.8–5.5 μm) is real or is due to probe response.

Contrail identification was accomplished through a combi-

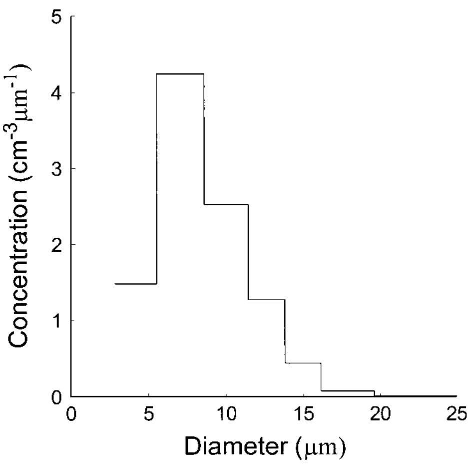

Figure 1. Particle size distribution for lone contrail (*F*) from FSSP data.

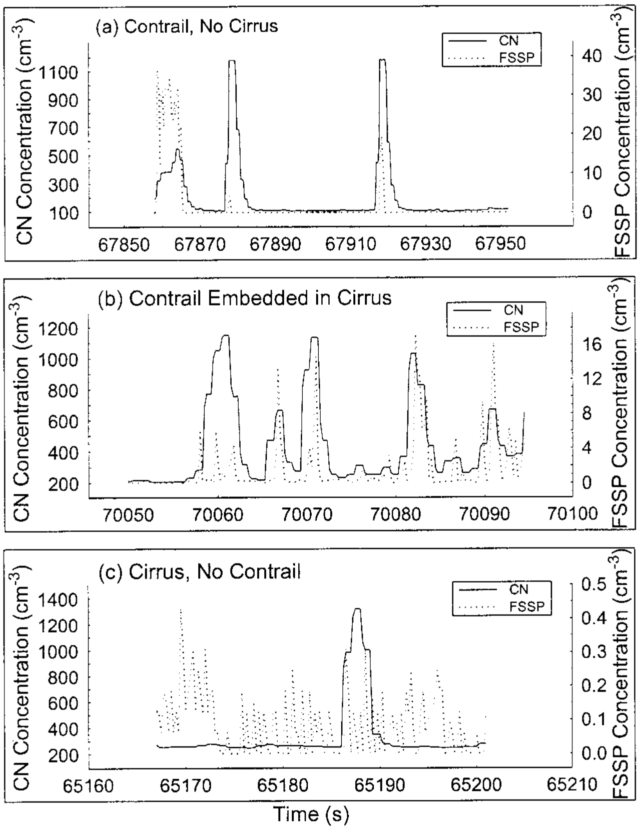

Figure 2. Time series of CN and FSSP concentrations through Citation exhaust plume: (a) in visually distinct contrails, (b) in contrail embedded within natural cirrus, and (c) crossing plume in natural cirrus with no apparent contrail particles.

nation of FSSP and condensation nuclei (CN) data based on penetrations of several contrail clouds which were visually distinct. It was important to establish objective criteria for identification because, while flying, it was not always possible to visually determine whether the aircraft was in fact traversing a contrail cloud. It was found that these contrail signatures appeared as coincident peaks in CN and FSSP concentrations. In addition, FSSP mean diameters in these contrails were small, of the order of 7–10 μm. It was then possible to search the entire Citation data sets from FIRE and ARM to identify as possible contrails the data segments where FSSP concentrations exceeded 1 cm^{-1} (with small mean diameters) coincident with increases in CN concentrations of at least 25%. Figure 2 illustrates the contrail FSSP and exhaust plume CN signature for three different conditions. Figure 2a shows a series of penetrations through Citation contrails which occurred in clear air and were identified visually in flight. The CN counter reached the maximum of its set range (>1275 cm^{-3}), and FSSP concentrations approached 40 cm^{-3} (mean diameter 7 μm). These data are summarized in Table 2 as contrail samples G2, J1, and J2. Figure 2b shows data from a flight segment in natural cirrus where the Citation was flying along its own exhaust track. This embedded contrail sample (N) was identified through use of the post hoc criteria, with CN peak values >1100 cm^{-3} and FSSP >17 cm^{-3} (mean diameter 14 μm). Figure 2c shows the FSSP and CN data in natural cirrus. There is no contrail cloud apparent in the FSSP (peak <0.5 cm^{-3}, mean diameter 33 μm), although there is evidence of the Citation exhaust in the CN (peak >1300 cm^{-3}) as the aircraft crossed its own plume.

This identification procedure may have excluded aged contrails where particle growth and plume dilution could have masked the contrail signature. It is also possible that this pro-

Table 2. Summary of Contrail Properties

Date UTC	Time UTC	ID	Temp, °C	Pressure, hPa	Altitude, km	Cloud	Citation	Conc Max, cm^{-3}	Conc Ave, cm^{-3}	Size Ave, μm	Age, s	Width, m	ΔCN, cm^{-3}
11/22/91	34003	A	−53.6	250	10.5	Y	Y	46.7	26.5	9.4	694		na
11/25/91	172147	B	−49.1	292	9.4	Y	Y	5.7	3.9	10.5	233	137	na
11/26/91	180312	C	−51.4	288	9.4	Y		15.7	11.6	7.5			35
	180932	D	−51.4	288	9.4	Y	Y	1.0	0.3	25.2	2640	2377	287
	182002	E	−54.6	270	9.8	Y		11.9	7.1	14.2			47
	182721	F	−57.0	260	10.1			31.1	20.6	8.2			194
	184819	G1	−59.4	250	10.3		Y	19.7	12.5	7.2	732	225	347
	185057	G2	−58.9	251	10.3		Y	37.1	25.7	7.5	907	360	524
	184834	H1	−59.3	250	10.3			15.9	6.8	11.8			55
	185023	H2	−59.0	250	10.3			25.5	11.5	10.0			78
	184856	I1	−59.2	250	10.3			5.3	3.7	17.6			79
	185014	I2	−59.1	251	10.3			8.2	4.6	17.0			106
	185116	J1	−58.9	251	10.3		Y	4.3	3.4	5.7	187	30	>1275
	185156	J2	−58.9	251	10.3		Y	19.4	14.5	6.8	254	15	>1275
	185849	K1	−59.2	251	10.3			22.1	8.8	10.5			93
	190036	K2	−57.3	260	10.1			7.1	5.3	9.8			46
	190046	L	−57.1	261	10.1			1.6	0.7	20.7			154
11/28/91	191535	M	−47.4	262	10.1			69.0	63.1	9.4			963
	192739	N	−52.9	238	10.7	Y	Y	17.3	5.1	13.6	310		940
11/30/91	162603	O	−54.2	217	11.3		Y	31.2	16.1	8.1	179	230	340
	163259	P	−54.4	217	11.3	Y	Y	31.6	18.8	6.8	178	66	385
12/5/91-2	184745	Q	−56.2	217	11.3	Y		12.2	8.0	9.3			55
	185818	R	−61.5	196	11.9			4.3	2.4	14.2			30
4/18/94-1	15829	S	−65.3	180	12.4		Y	9.5	3.1	8.5	244		1100
	20236	T	−65.2	180	12.4		Y	13.0	8.4	7.4	206	172	365
4/19/94	30744	U	−65.8	179	12.5		Y	11.2	5.0	8.7	NA		5714

Contrail width not available for contrails *A*, *N*, *S*: Citation flew along contrail. Read 11/21/91 as November 21, 1991. Conc, concentration.

Table 3. Contrail Properties by Age and Cloudiness

Property	Age, min			Cloud	Clear
	3–6	10–15	44		
Max conc, cm^{-3}	17.9 (8)	34.3 (3)	1.0 (1)	19.2 (8)	18.6 (18)
Mean conc, cm^{-3}	9.2 (8)	21.6 (3)	0.3 (1)	10.2 (8)	12.0 (18)
Mean diameter, μm	8.4 (8)	7.9 (3)	25.2 (1)	12.1 (8)	14.2 (18)
ΔCN, cm^{-3}	819 (7)	436 (2)	287 (1)	292 (6)	461 (18)
Contrail width, m	108 (6)	293 (2)	2377 (1)		

Numbers in parentheses are number of samples.

cedure included as contrails some regions of natural cirrus which contained elevated CN concentrations. (However, none of the samples that were identified as contrails were associated with elevated CN regions of more than 2 km in horizontal extent.) The ages of the sampled contrails produced by the Citation were determined from flight track crossings by drifting the aircraft track with the wind. The angle and time in contrail also made it possible to determine the width of the contrail. The ages and widths of contrails from other aircraft could not be determined.

3. Contrail Microphysical Properties

Table 2 provides a summary of the contrails sampled in this study. All but contrail M occurred at temperatures and altitudes which required ambient humidities less than ice saturation according to *Appleman* [1953]. Contrail M would have required a relative humidity of ~70% relative to water or 110% relative to ice saturation. The concentration and size information provided by the FSSP shows that on average, these contrails contained particles of mean diameter of the order of 10 μm in concentrations exceeding 10,000 L^{-1}. These values are similar to those measured in SUCCESS by *Goodman et al.* [1998]. The highest sampled concentration was 69,000 L^{-1}. This is in contrast with observations of contrails reported by *Gayet et al.* [1996a], where the maximum concentration observed was 820 L^{-1} and mean diameters ranged from 34 to 47 μm. The measurements by *Gayet et al.*, however, were limited to particles larger than 25 μm and the contrails existed at warmer temperatures where more water vapor was available for particle growth. When Gayet et al. [1996b] considered the FSSP data, they found concentrations up to 1500 L^{-1}.

The general variability in the contrail properties in Table 2 is likely the result of several factors, including the environmental conditions under which the contrails were formed, the aircraft type and power setting, measurement uncertainties of the FSSP, and the position within the contrail where the Citation was sampling. Again, these penetrations were mostly inadvertent and were not necessarily made through the center of the contrail cloud.

Several stratifications of the contrail characteristics are presented in Table 3. The contrails produced by the Citation were observed to spread laterally with time as a consequence of turbulence. An exception is contrail J which may have been dissipating. Interestingly, the concentrations of particles detected by the FSSP generally increased with age through 15 min. It is postulated that this was the result of growth of ice particles to detectable size as ambient water vapor was entrained into the plume (as in the work of *Heymsfield et al.* [1998]). During this same time period the mean aerosol perturbation (ΔCN) decreased through dilution and perhaps aggregation and scavenging processes. The oldest contrail contained the largest and fewest ice crystals.

A comparison is also made between contrails occurring in clear air and those embedded within natural cirrus. Column 5 in Table 3 is for a subset of contrails where 1D-C measurements of natural ice concentrations exceeded 10 L^{-1}. There appears to be little difference in ice particle concentrations or sizes between embedded and nonembedded contrails. In terms of aerosol perturbation (ΔCN), there is a tendency for the embedded contrails to have lower values above background than contrails formed in clear air. This could be due to scavenging by the natural cirrus ice particles, although the total surface area of the contrail particles is several times that of the natural cirrus.

To examine the possible effects of the contrails on natural cirrus, a subset of five embedded contrails was selected for those occurring within natural cirrus with 1D-C concentrations of at least 10 L^{-1}. Figure 3 shows a comparison of particle spectra in the embedded contrail and in the cirrus alone. Little difference between the two is evident, within the measurement uncertainties of the FSSP, except for the addition of particles <30 μm in the cirrus with embedded contrail. The contrail and cirrus spectra are very similar to those reported by *Lawson et al*. [1998]. The ambient cirrus in the Lawson paper shows more small particles than ours, though this difference could easily be due to natural variability. Lack of direct comparison of the suite of instruments described in the Lawson paper with ours limits further analysis.

A summary comparison for the five cloudy contrails shows 1D-C concentrations and mean sizes of 15.9 L^{-1} and 92 μm (15.7 L^{-1} and 92 μm) for natural cirrus (embedded contrails). FSSP values were 0.2 and 31.6 cm^{-3} (7.2 L^{-1}, 11.2 μm) for the natural (embedded) samples. From these values it appears that these contrails had little, if any, effect on the numbers and sizes of particles large enough to be detected by the 1D-C, i.e., particles larger than 40 μm maximum dimension. The main effect of the contrail on natural cirrus was to add small parti-

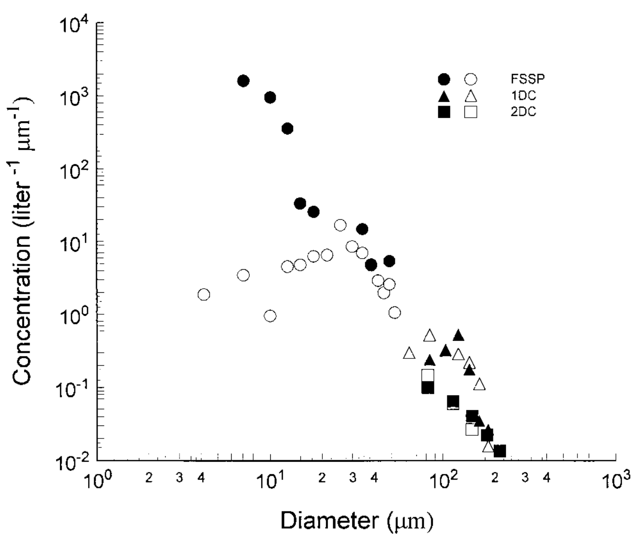

Figure 3. Particle size distribution for embedded contrail (Q) and natural cirrus, from FSSP, 1D-C, and 2D-C data. Solid symbols represent the contrail. The number of data points in the two curves differ because of the presence of zero counts in some probe channels.

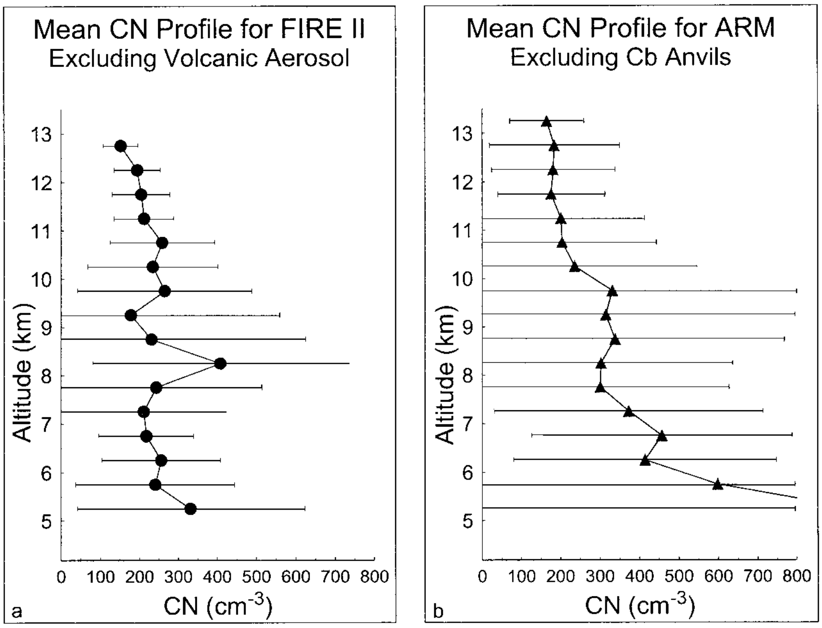

Figure 4. Vertical distributions of mean CN concentrations for the (a) FIRE II and (b) ARM projects. Error bars show standard deviation of values. Lines connecting data points are shown only as a visual guide for the reader.

cles. Aggregation, evaporation, and growth of natural cirrus did not appear to happen, at least prior to the times of these samples.

4. Effects of Exhaust Aerosols

An examination of CN and cloud microphysical data may provide some insight to the effects of aircraft exhaust on natural cirrus generation. *Karcher et al.* [1996] have suggested that exhaust aerosol may remain active in the atmosphere as cloud condensation or ice nuclei subsequently affect the formation of cirrus at a later time. Although the CN counter does not provide any information as to the origin, composition, or ice/water nucleating properties of aerosol, it does detect the presence of soot and other exhaust aerosol. Thus the CN data may be used to detect the presence of aircraft exhaust plumes or traffic corridors. A search for possible exhaust/cloud interactions was made by examining known samples of Citation exhaust and also looking at general distributions of aerosol and clouds.

There are, of course, atmospheric conditions where jet aircraft do not produce persistent contrails because the atmosphere is too warm or too dry, so there were times when the Citation penetrated its own exhaust plume and no contrails were present. However, there were also six occasions when the CN plume from the Citation was found embedded within natural cirrus but with no indications of contrail cloud particles present in the FSSP data. An example is shown in Figure 2c. This is in contrast to the embedded contrail cases discussed in section 3. These no-contrail cases occurred in plumes that were 3–7 min old, at temperatures of −47°C to −53°C, and in particle concentrations of a few to over 100 L^{-1}. Unfortunately, because of a lack of reliable relative humidity data, it is not known whether Appleman criteria were satisfied. Perhaps the natural cirrus was beginning to dissipate and the relative humidity had dropped below ice saturation or, for that temperature and pressure, the ambient humidity was insufficient for contrails to persist. These samples do indicate, however, that jet aircraft do not always produce persistent contrails when flying through regions of natural cirrus. There was no detectable difference in the character of the cirrus in or out of the plume.

The data from all flights of the FIRE and ARM programs were examined to look for any statistical correlation between CN spatial distributions and cloud properties. Figure 4 shows the mean vertical distributions of CN sampled during these two projects, excluding days when volcanic aerosols were present in FIRE and when thunderstorms had pumped boundary layer air aloft during ARM. There is a suggestion of elevated CN concentrations in the altitude range of 8–11 km which could possibly be attributed to aircraft exhaust. This represents flight altitudes of ~26,000–36,000 feet, which includes typical cruising altitudes for the busy jet route corridors in the central United States. It is also possible, though, that vertical transport processes may have been responsible for lifting relatively dirty boundary layer air to these heights [*Talbot et al.*, 1998].

If the aircraft exhaust aerosols do remain active as cloud-forming nuclei and are traceable by CN measurements, perhaps CN concentrations would be correlated with cloud microphysical properties. However, regressions of cloud ice particle sizes and concentrations with CN concentrations showed no significant correlation. (An example is shown in Figure 5.) It is not known whether this was because the exhaust aerosols were not active as cloud nuclei or that the bulk of the measured CN were not from aircraft exhaust. Thus we were not able to discern any effect of exhaust aerosols on natural cirrus clouds in this limited study.

5. Radiative Properties

The radiative influence of contrails is complicated by the associated irregular geometry, partial sky coverage, and pres-

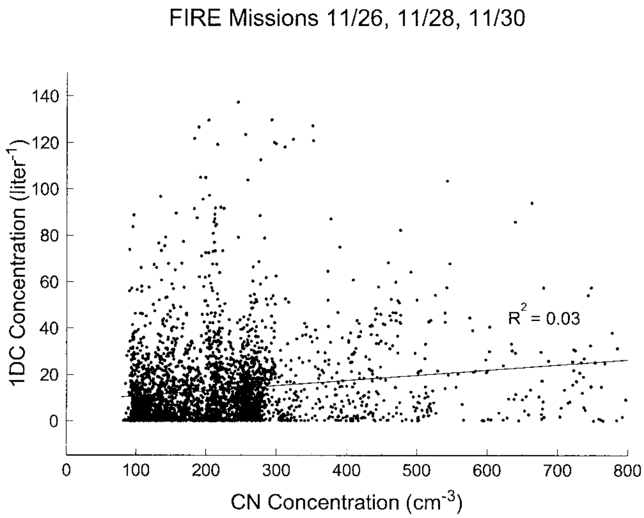

Figure 5. Scatterplot of cirrus ice particle concentrations versus CN concentrations, with linear best fit correlation.

ence of natural cirrus. Any claims about the total radiative impact of contrails under a variety of conditions are unfortunately not forthcoming at present, though we have performed some estimates of the infrared properties of contrail characterized by size distributions in Figures 1 and 3 and have compared these estimates with natural cirrus characterized by the size distribution in Figure 3. *Arnott et al.* [1995] have performed infrared extinction measurements (2–18 μm) on laboratory ice clouds that have distributions similar to contrails. These measurements have subsequently been modeled by a variety of algorithms, and it was found that anomalous diffraction theory for spheres could be adapted to reasonably simulate the lab results with proper choice of an algorithm to convert a spherical ice particle to a hexagonal crystal.

The procedures used to estimate the infrared properties were as follows: The maximum dimension for a crystal is given by D and is expressed in micrometers. The volume of a plate ice crystal is taken to be

$$V = 2.3D^{2.475}\ (\mu\text{m}^3), \tag{1}$$

and the average projected area under random orientation is calculated by [*Pruppacher and Klett*, 1980].

$$P = 0.75D\{3^{1/2}D/4 + 2.02D^{0.449}\}\ (\mu\text{m}^2) \tag{2}$$

The equivalent diameter of a particle is taken to be

$$D_e = V/P, \tag{3}$$

and the radius of an equivalent sphere is

$$R_s = 0.75D_e. \tag{4}$$

(Note that this relationship is consistent for the special case of a spherical particle.) This value of R_s is then used by *van de Hulst*'s [1981] anomalous diffraction equation for a sphere to obtain the single-particle absorption and scattering efficiencies q_{abs} and q_{ext} for a particular wavelength and associated ice refractive index [from *Warren*, 1984]. The absorption coefficient B_{abs} (dimensions of inverse distance) is then obtained as an integral over the size distribution

$$B_{\text{abs}} = \int P(D)q_{\text{abs}}(\lambda, D)\ N(D)\ dD, \tag{5}$$

where $N(D)$ is the number of particles per unit volume per size interval having size between D and $D + dD$. A similar procedure is followed for B_{ext}, the extinction coefficient. Then cloud transmission is expressed as

$$T(\lambda) = \exp\ (-B_{\text{ext}}L), \tag{6}$$

cloud emissivity as

$$e(\lambda) = [1 - \exp\ (-B_{\text{abs}}L)], \tag{7}$$

and cloud radiance for an overhead cloud as

$$L(\lambda) = B(T_c, \lambda)B_{\text{abs}}[1 - T(\lambda)]/B_{\text{ext}}, \tag{8}$$

where T_c is the cloud temperature and B is blackbody radiance for this temperature. This simple relation for radiance assumes a homogeneous, isothermal cloud, and it takes into account the possibility that radiance emitted at one place in the cloud may be removed from the forward direction through extinction. The single-scattering approximation for cloud transmission is likely to be reasonable only when $B_{\text{sca}}L < 1$; that is, the scattering optical depth is less than unity. The approximate nature of this approach may be objectionable because it does not use a sophisticated single-particle scattering theory, or multiple scattering for transmission, and it does not incorporate contributions from gases. However, it is quite useful for isolating and comparing the IR properties of various ice-containing clouds.

Simulated infrared radiative properties of natural cirrus and cirrus with an embedded contrail (see Figure 3) are presented in Figure 6 (1 km cloud thickness at −60°C), and those of an

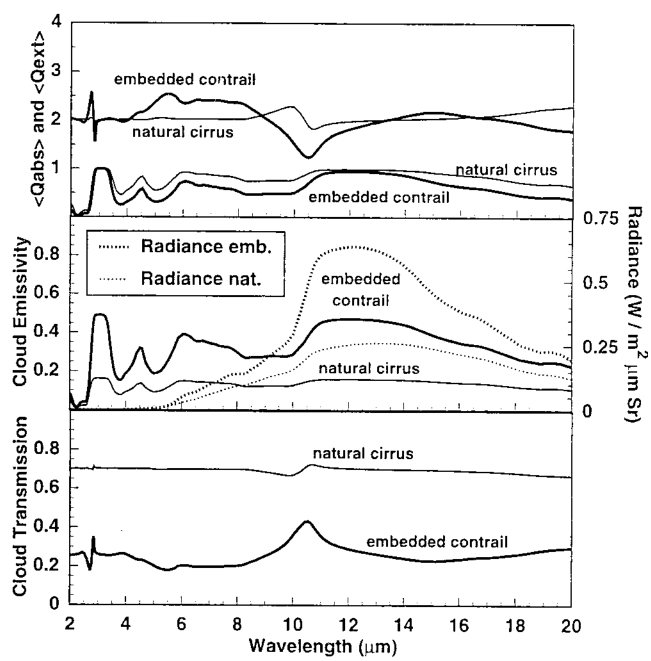

Figure 6. Infrared radiative properties of natural cirrus and cirrus with an embedded contrail. Thin lines show values for natural cloud. In the top panel, the extinction and absorption efficiencies are shown by the top two curves and bottom two curves, respectively.

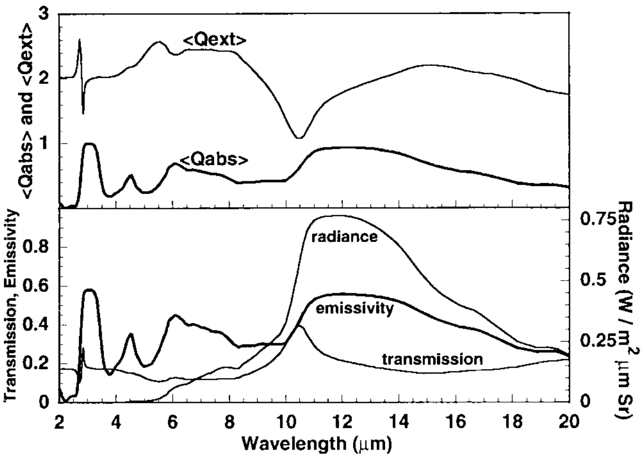

Figure 7. Infrared radiative properties of a lone contrail.

isolated contrail described by the size distribution in Figure 1 are presented in Figure 7 (500 m cloud thickness and −57°C). Recall that the embedded contrail cirrus is very similar to the natural cirrus concerning the crystal content beyond 50 μm, though the embedded contrail cirrus has about 3 orders of magnitude greater numbers of small crystals. The top panels in Figures 6 and 7 display the integrated extinction and absorption efficiencies (cross sections divided by the total projected area). Note that lone and embedded contrail cirrus have considerably more spectral variation in these efficiencies than natural cirrus. This is a direct consequence of the numbers of small crystals. The middle panel in Figure 6 compares the emissivity and emission at the cloud-embedded contrail and natural cirrus. Note that the emissivity and emission by embedded contrail cirrus is greater than that of natural cirrus as one would expect because of the higher mass content of embedded contrail. The bottom panel in Figure 6 indicates the embedded contrail has greater spectral variation in cloud transmission (with the relative maximum near 10.5 μm due to the Christiansen effect discussed by *Arnott et al*. [1995]) than natural cirrus, and certainly less overall transmission. Comparison of the bottom panel in Figure 7 with the middle and bottom panels in Figure 6 provides some evidence that the spectral variation of cloud emissivity, emission, and transmission is largely due to the presence of small ice crystals and that emission and transmission amounts are also considerably driven by the small crystals. It is likely that the embedded contrail cirrus and contrail cirrus will strongly influence the solar albedo as well as the direct and diffuse radiance amount arriving at the ground.

6. Conclusion

These findings suggest that contrails should not be treated as natural cirrus when modeling their climatic impact. Contrails found in clear air generally have more numerous and smaller ice crystals than natural cirrus. Natural cirrus with embedded contrails are likely to be describable as a cloud combination of these components, with little or no alteration of the natural cirrus by the contrail. The strong spectral variation of infrared transmission and emission by contrails or natural cirrus with embedded contrail is likely due to the small crystals ($<$50 μm) present in large number ($\sim$$10^5$ per liter).

Acknowledgments. The work of M. Poellot was supported by NASA grant NAG 5-2699 and that of W. P. Arnott and J. Hallett by NASA grant NAG 1-1707.

References

Appleman, H., The formation of exhaust condensation trails by jet aircraft, *Bull. Am. Meteorol. Soc*., *34*, 14–20, 1953.

Arnott, W. P., Y. Y. Dong, and J. Hallett, Extinction efficiency in the IR (2 μm to 18 μm) of laboratory ice clouds: Observations of scattering minima in the Christiansen bands of ice, *Appl. Opt*., *34*, 541–551, 1995.

Baumgardner, D., and W. A. Cooper, Airborne measurements in jet contrails: Characterization of the microphysical properties of aircraft wakes and exhausts, *Tech. Rep. DLR-Mitt. 94-06*, 496 pp., Dtsch. Forsch. für Luft und Raumfahrt, Cologne, Germany, 1994.

Baumgardner, D., J. Dye, and B. Gandrud, Calibration of the forward scattering spectrometer probe used on the ER-2 during the Airborne Antarctic Ozone Experiment, *J. Geophys. Res*., *94*, 16,475–16,480, 1989.

Baumgardner, D., J. Dye, and B. Gandrud, Interpretation of measurements made by the forward scattering spectrometer probe (FSSP-300) during the Airborne Arctic Stratospheric Expedition, *J. Geophys. Res*., *97*, 8035–8046, 1992.

Changnon, S., R. Semonin, and W. Wendland, Effect of contrail cirrus on surface weather conditions in the Midwest—Phase I, 141 pp., final report, NSF grant NSF ATM 78-09568, Ill. State Water Surv., Champaign, 1980.

Gardiner, B. A., and J. Hallett, Degradation of in-cloud forward scattering spectrometer probe measurements in the presence of ice particles, *J. Atmos. Oceanic Technol*., *2*, 171–180, 1985.

Gayet, J., G. Febvre, G. Brogniez, H. Chepfer, W. Renger, and P. Wendling, Microphysical and optical properties of cirrus and contrails: Cloud field study on 13 October 1989, *J. Atmos. Sci*., *53*, 126–138, 1996a.

Gayet, J., G. Febvre, and H. Larsen, The reliability of the PMS FSSP in the presence of small ice crystals, *J. Atmos. Oceanic Technol*., *13*, 1300–1310, 1996b.

Goodman, J., R. F. Pueschel, E. J. Jensen, S. Verma, G. V. Ferry, S. D. Howard, S. A. Kinne, and D. Baumgardner, Shape and size of contrail ice particles, *Geophys. Res. Lett*., *25*(9), 1327–1330, 1998.

Gothe, M., and H. Grassl, Satellite remote sensing of the optical depth and mean crystal size of thin cirrus and contrails, *Theor. Appl. Climatol*., *48*, 101–113, 1993.

Heymsfield, A., and C. Platt, A parameterization of the particle size spectrum of ice clouds in terms of the ambient temperature and the ice water content, *J. Atmos. Sci*., *41*, 846–855, 1984.

Heymsfield, A. J., R. P. Lawson, and G. W. Sachse, Growth of ice crystals in a precipitating contrail, *Geophys. Res. Lett*., *25*(9), 1335–1338, 1998.

Hudson, J. G., and Y. Xie, Cloud condensation nuclei measurements in the high troposphere and in jet aircraft exhaust, *Geophys. Res. Lett*., *25*(9), 1395–1398, 1998.

Jensen, E. J., O. B. Toon, R. F. Pueschel, J. Goodman, G. W. Sachse, B. E. Anderson, K. R. Chan, D. Baumgardner, R. C. M.-Lye, Ice crystal nucleation and growth in contrails forming at low ambient temperatures, *Geophys. Res. Lett*., *25*(9), 1371–1375, 1998.

Johnson, S., J. McQuigg, and T. Rothrock, Temperature modification and costs of electric power generation, *J. Appl. Meteorol*., *8*, 919–926, 1969.

Karcher, B., T. Peter, U. M. Biermann, and U. Schumann, The initial composition of jet condensation trails, *J. Atmos. Sci*., *53*, 3066–3083, 1996.

Knollenberg, R. G., Measurements of the growth of the ice budget in a persisting contrail, *J. Atmos. Sci*., *29*, 1367–1374, 1972.

Knollenberg, R., K. Kelly, and J. Wilson, Measurements of high number densities of ice crystals in the tops of tropical cumulonimbus, *J. Geophys. Res*., *98*, 8639–8664, 1993.

Kuhn, P. M., Airborne observations of contrail effects on the thermal radiation budget, *J. Atmos. Sci*., *27*, 937–942, 1970.

Lawson, R. P., A. J. Heymsfield, S. M. Aulenbach, and T. L. Jensen, Shapes, sizes, and light scattering properties of ice crystals in cirrus and a persistent contrail during SUCCESS, *Geophys. Res. Lett*., *25*(9), 1331–1334, 1998.

Liou, K. N., S. C. Ou, and G. Koenig, An investigation of the climatic effect of contrail cirrus, in *Air Traffic and the Environment—*

Background, Tendencies, and Potential Global Atmospheric Effects, edited by U. Shcumann, pp. 154–169, Springer-Verlag, New York, 1990.

Minnis, P., D. F. Young, D. P. Garber, L. Nguyen, W. L. Smith Jr., and R. Palikonda, Transformation of contrails into cirrus during SUCCESS, *Geophys. Res. Lett.*, *25*(8), 1157–1160, 1998.

Pueschel, R. F., J. Hallett, A. W. Strawa, S. D. Howard, G. V. Ferry, T. Foster, and W. P. Arnott, Aerosol and cloud particles in tropical cirrus anvil: Importance to radiation balance, *J. Aerosol Sci.*, *28*, 1123–1136, 1997.

Sassen, K., Contrail-cirrus and their potential for regional climate change, *Bull. Am. Meteorol. Soc.*, *78*, 1885–1903, 1997.

Sassen, K., M. Griffin, and G. Dodd, Optical scattering and microphysical properties of subvisual cirrus clouds, and climatic implications, *J. Appl. Meteorol.*, *28*, 91–98, 1989.

Schumann, U., J. Ström, R. Busen, R. Baumann, K. Gierens, M. Krautstrunk, F. P. Schröder, and J. Stingl, In situ observations of particles in jet aircraft exhausts and contrails for different sulfur-containing fuels, *J. Geophys. Res.*, *101*, 6853–6869, 1996.

Smith, W. L., S. Ackerman, H. Revercomb, H. Huang, D. H. DeSlover, W. Feltz, L. Gumley, and A. Collard, Infrared spectral absorption of nearly invisible cirrus clouds, *Geophys. Res. Lett.*, *25*(8), 1137–1140, 1998.

Talbot, R. W., J. E. Dibb, and M. B. Loomis, Influence of vertical transport on free tropospheric aerosols over the central USA in springtime, *Geophys. Res. Lett.*, *25*(9), 1367–1370, 1998.

Toon, O. B., and R. C. M.-Lye, Subsonic Aircraft Contrail and Cloud Effects Special Study (SUCCESS), *Geophys. Res. Lett.*, *25*(8), 1109–1112, 1998.

Twohy, C. H., and B. W. Gandrud, Electron microscope analysis of residual particles from aircraft contrails, *Geophys. Res. Lett.*, *25*(9), 1359–1362, 1998.

van de Hulst, H. C., *Light Scattering by Small Particles*, pp. 173–194, Dover, Mineola, N. Y., 1981.

Warren, S. G., Optical constants of ice from the ultraviolet to the microwave, *Appl. Opt.*, *23*, 1206–1225, 1984.

Wendland, W., and R. Semonin, Effect of contrail cirrus on surface weather conditions in the Midwest—Phase II, final report, NSF ATM 8008812, Ill. State Water Surv., Champaign, 95 pp., 1982.

Zhang, Z., and Y. H. Liu, Performance of TSI 3760 condensation nuclei counter at reduced pressures and flow rates, *Aerosol Sci. Technol.*, *15*, 228–238, 1991.

M. R. Poellot, Department of Atmospheric Sciences, University of North Dakota, P. O. Box 9006, Grand Forks, ND 58201. (poellot@aero.und.edu)

W. P. Arnott and J. Hallett, Atmospheric Research Center, Desert Research Institute, Reno, NV 89506.

(Received May 6, 1998; revised February 5, 1999;
accepted February 11, 1999.)